4) Peak current rates of rise, if assumed to be produced by CG strikes, range from 0.6×10^{10} to 1.6×10^{11} A s^{-1}. These values are close to those estimated by Weidman and Krider[2] at ground level.

When a return stroke of a CG flash that started at the ground with a peak current of 200 kA and a current rate of rise of 10^{11} A s^{-1} reaches an airplane at flight altitude, its peak current and rate of rise will be much smaller. Applying the exponential decrease of the return stroke light intensity[9] [(exp) $-0.6n$, where n is the altitude of the airplane in km] to the variation of the peak current in return strokes with altitude results in a peak return stroke current of 10 kA at 5 km altitude, which is in the range of values measured on the F-106B. The rate of current rise from the peak detector measurements is, however, much greater than that expected with the exponential decrease of its maximum values with altitude.

When a CG strike initiates on the airplane, the peak current is expected to be at its maximum on the airplane, rather than at the ground, whereas the highest rate of rise may occur anywhere along a negative stepped leader channel. The maximum values of peak currents and rate of rise measured on the F-106B were 54 kA and 3.8×10^{11} A s^{-1}, respectively, during the flights with non-CG strikes to the airplane.[8] Since the majority of strikes to the F-106B were triggered on the airplane,[10] it is reasonable to suggest that the largest peak values of currents and rates of rise characterize triggered strikes rather than intercepted return strokes of CG flashes. The SAE criteria on peak current rates of rise, although based on a worst-case assumption of the first return stroke attachment to the airplane with peak values equal to those measured at the ground, match in-flight measurements of current rates of rise measured during triggered strikes. The SAE criteria on peak currents, however, far exceed the predicted values of return stroke currents at flight altitudes and are also much greater than the values measured during triggered strikes.

Acknowledgments

This work was supported in part by NASA Grant RM2A1K85. The authors are grateful to John Gerlach of NASA Wallops Flight Facility for his help in data reduction.

References

[1]Uman, M., *The Lightning Discharge,* Academic, Orlando, FL, 1987.

[2]Weidman, C. D., and Krider, E. P., "The Fine Structure of Lightning Return Stroke Wave Forms," *Journal of Geophysical Research,* Vol. 83, 1978, p. 6239–6247.

[3]SAE Committee AE4L, "Recommended Draft Advisory Circular: Protection of Aircraft Electrical/Electronic Systems Against Indirect Effects of Lightning," Society of Automotive Engineers, Committee Rept. AE4L-87-3, Feb. 1987.

[4]Idone, V. P., and Orville, R. E., "Correlated Peak Relative Light Intensity and Peak Current in Triggered Lightning Subsequent Return Strokes," *Journal of Geophysical Research,* Vol. 90, 1985, pp. 615–6164.

[5]Orville, R. E., Henderson, R. W., and Bosart, L. F., An East Coast Lightning Detection Network," *Bulletin of the American Meteorologic Society,* Vol. 64, No. 9, 1983, pp. 1029–1037.

[6]MacGorman, personal communication, 1989.

[7]Plumer, J. A., Rasch, N. O., and Glynn, M. S., "Recent Data From the Airlines Lightning Strike Reporting Project," *Journal of Aircraft,* Vol. 22, 1985, pp. 429–433.

[8]Pitts, F. L., Lee, L. D., Perala, R. A., and Rudolph, T. H., "New Methods and Results for Quantification of Lightning-Aircraft Electrodynamics," NASA TP-2737, June 1987.

[9]Jordan, D. M., and Uman, M. A., "Variation in Light Intensity with Height and Time from Subsequent Lightning Return Strokes," *Journal of Geophysical Research,* Vol. 88, 1983, pp. 6555–6562.

[10]Mazur, V., "A Physical Model of Lightning Initiation on Aircraft in Thunderstorms," *Journal of Geophysical Research,* Vol. 94, 1989, pp. 3326–3340.

Freestream Turbulence Effects on Airfoil Boundary-Layer Behavior at Low Reynolds Numbers

Richard M. Howard*
and
David W. Kindelspire†
Naval Postgraduate School, Monterey, California

Introduction

WITH the increased interest in the application of remotely piloted vehicles (RPVs) comes the need for a better understanding of the aerodynamic problems associated with airfoil performance at low Reynolds numbers. For airfoils in this regime, it is well known that transition from laminar to turbulent flow and flow separation are highly sensitive to the disturbance environment.[1] The formation of laminar separation bubbles at low Reynolds numbers, and their dependence on freestream disturbances, complicates the study of airfoil performance compared to flows at more conventional Reynolds numbers. Boundary-layer sensitivity to flowfield conditions often leads to varying results for identical airfoil models in different wind tunnels.[2] Mueller et al.[1] presented results from the addition of a wire mesh screen upstream of the wind-tunnel test section for which the turbulence intensity was raised from an ambient level of 0.08% to a level of 0.3%. The hysteresis associated with the laminar separation bubble on a Wortmann FX 63-137 airfoil in the lift and drag curves disappeared with the addition of the screen. Marchman[2] likewise found a reduction in the lift hysteresis for the Wortmann airfoil when the freestream turbulence level was raised from 0.02 to 0.2%. Both groups of investigators noted the dependence of the effect of a disturbance upon its frequency content.

Early investigators used empirical data to correlate freestream turbulence levels with the momentum thickness Reynolds number R_θ at transition.[3] Hall and Gibbings[3] discuss the earlier work of Hilsop,[4] who tested the effects of varying mesh grids upon transition location. Indications were that at the same turbulence intensity level, the larger mesh grid was less effective in promoting early transition. No correlation of the mesh size with turbulence length scale was given. Abu-Ghannam and Shaw[5] studied transitional behavior using six turbulence grids producing turbulence levels from 0.5 to 5%. Correlations were established between turbulence levels and the starting and ending values of R_θ during the transition process. Turbulence length scales were calculated from a time correlation, but it was noted that the effect of turbulence scale was small and therefore neglected.

Meier and Krep1in[6] considered the effects of grid-generated turbulence levels from 0.06 to 1%. By spectral analysis, they attempted to separate the effect of turbulence intensity from

Received July 5, 1989; revision received Aug. 30, 1989.

*Assistant Professor, Department of Aeronautics and Astronautics. Member AIAA.

‡Graduate Student; Lieutenant, U.S. Navy.

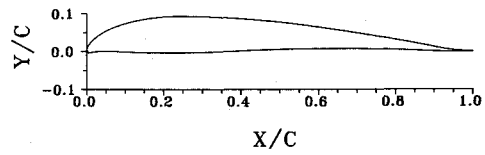

Fig. 1 Airfoil.

Table 1 Grid specifications[a]

Grid	M	d	M/d	Material
1	5.0	1.0	5	Wood
3	2.5	0.5	5	Wood
4	1.0	0.0625	16	Wire

[a]Dimensions in inches.

that of turbulence scale. It was noted that at a constant turbulence intensity, different grid dimensions and positions generated turbulence of different spectra, which resulted in different integral length scales. Maximum values of skin-friction coefficients were obtained at length scales on the order of the boundary-layer thickness, with a doubling of the length scale decreasing the skin-friction coefficient slightly. No effect of the turbulent structure on transition was considered, as the transition was artificially fixed in the experiment.

It was desired to conduct wind-tunnel experiments on the effect of turbulence length scales at elevated turbulence levels upon the transitional behavior of flow over an airfoil at a relatively low Reynolds number. Described in this Note are measured velocity profiles at nine stations along the airfoil surface for four conditions of turbulence intensities and length scales.

Experimental Procedure

The wind tunnel used for the experiments at the Naval Postgraduate School has a test section measuring 28 by 45 in., with a contraction ratio of approximately 10. The Reynolds number for the runs was 5×10^5. The airfoil model has a 10-in. chord and a 24-in. span and was mounted horizontally between vertical supports. The airfoil is shown in Fig. 1. The model was made from a helicopter tail rotor section and was filled and smoothed to contour. The coordinates as measured on a numerical milling machine are available from the first author. The model was mounted at an angle of attack of 6 deg. Velocity profiles were measured on the upper surface only. A three-dimensional traversing system moved a single-sensor hot-wire anemometer probe vertically through the boundary layer at different chord locations. The resolution of the traversing mechanism was 0.000125 in. An engineer's transit was used to observe the probe. The sensor could be accurately placed within 0.003 in. of the airfoil surface.

A set of four turbulence grids were constructed for the study. Results for the ambient (no grid) case and for three of the grids are presented here. The two larger-mesh grids (grids 1 and 3) were square-mesh, square-bar, biplanar grids, and the third (grid 4) was a square-mesh, round-wire grid. Table 1 contains grid specifications for the varying mesh sizes (M) and bar diameters (d). The grids were located at the downstream end of the contraction section of the settling chamber, 67 in. (6.7 chord lengths) upstream of the leading edge of the airfoil model. Turbulence grids of this type (the first two) have been found to successfully generate nearly isotropic turbulence.[7,8] With this grid design, the longitudinal turbulence intensity is about 5% greater than the lateral and transverse components.[9] This relation was used to extract the longitudinal component using a single hot-wire sensor to measure the component in the freestream plane. Figure 2a shows the measured intensities for the three grids plotted against distance from the grids. Turbulence levels at the airfoil were 3.5, 1.9, and 0.5% for grids 1, 3, and 4 respectively. The ambient turbulence level in the test section at the test Reynolds number was 0.23%—not a low value, but typical for closed-circuit wind tunnels.

Meier[10] describes a method for correlating the decay of the turbulence intensity with the distance downstream of a turbulence-generating grid. Hancock and Bradshaw[8] and Castro[9] link the turbulence dissipation length scale L_e with the decay of turbulence intensity. Therefore, length scales representative of the turbulent dissipation eddies can be estimated from the turbulence-intensity measurements.

For grid-generated turbulence, the intensity decreases as

$$[(u'/U)^2]^{-0.8} = A(x/M - B) \tag{1}$$

where u' is the rms of the streamwise fluctuating velocity component, U is the streamwise mean velocity, x is the streamwise coordinate, and A and B are constants to be determined for each grid.[9] The turbulent dissipation length scale is related to the intensity[9] by

$$U[d(u'^2)/dx] = -(u')^{3/2}/L_e \tag{2}$$

giving length scales varying with downstream distance as

$$L_e/M = 0.8[A^{-0.625}][x/M - B]^{0.375} \tag{3}$$

Figure 2b indicates the dissipation length scales for the three grids. Note that the representative size increases gradually with downstream distance, due to the rapid dissipation of the smaller scales with viscosity. Length scales were estimated to be 1.85, 1.05, and 0.25 in. at the airfoil for grids 1, 3, and 4, respectively.

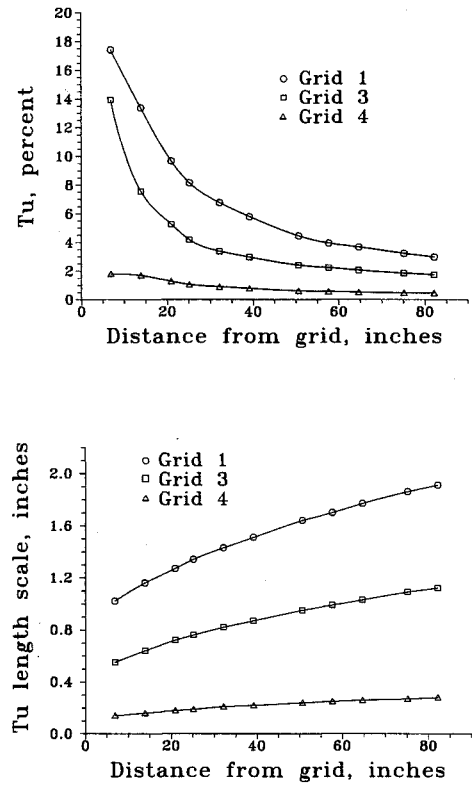

Fig. 2 Turbulence characteristics downstream from grids: a) intensity, b) length scales.

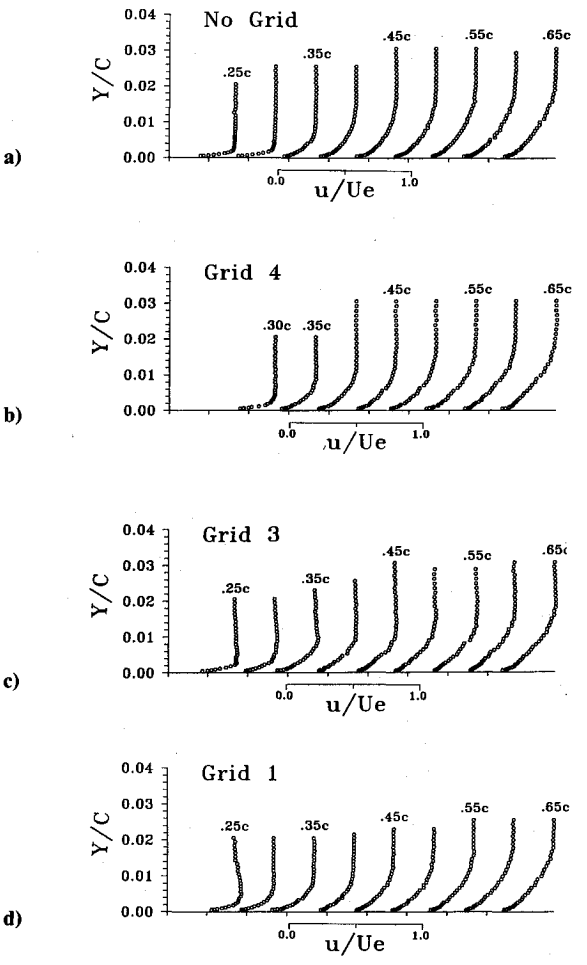

Fig. 3 Mean velocity profiles: a) no grid, b) grid, 4 c) grid 3, and d) grid 1.

Results

Boundary-layer data were collected at nine airfoil stations from 25 to 65% chord. Data are presented as mean boundary-layer velocity profiles, and will be discussed in order of increasing freestream turbulence intensity and scale.

Mean velocity profiles for the four cases are shown in Fig. 3. Tick marks on the x axis, reference points for the profiles, represent velocity levels of one-half the boundary-layer-edge value. Each velocity profile has been shifted to the right 0.3 times the edge velocity. The boundary-layer edge was taken to be the location at which the velocity reached a constant level or began decreasing to the freestream value.

Figure 3a shows mean profiles for the ambient condition. The boundary layer appears to be laminar up to the 30% chord (0.30c) location, as can be noted by the linear velocity gradient near the surface. At 35% chord, the profile takes on the fuller profile shape of a turbulent boundary layer, and begins to thicken at a much greater rate. The normalized boundary-layer height y/c can be estimated to be 0.015 at 45% chord and 0.020 at 65% chord.

Profiles for grid 4, the small wire-mesh grid, are shown in Fig. 3b. No profile is available at 25% chord due to probe breakage. At 30% chord, the profile is linear near the surface, indicating laminar behavior, but in the outer layer, the profile is rounded, indicating a transitional state. This is confirmed by the level of turbulence intensity (not shown) near the surface for the two cases; for the no-grid case, a level of 2.5% exists, whereas for grid 4, the intensity has reached a maximum of 7%. The thickness at 65% chord is about 0.024 in., showing a growth of about 20% over the no-grid case.

The profiles for grids 3 and 1, the large-mesh grids, are shown in Figs. 3c and 3d. For grid 3, the flow appears laminar at 25% chord and turbulent at 30% chord. For grid 1, the largest mesh grid, the flow appears already turbulent by 25% chord. Of interest is the boundary-layer thicknesses for these two cases. At 45% chord, the boundary-layer heights are about 0.012, slightly less than for the no-grid and grid 4 cases; at 65% chord, the heights are about 0.018 and 0.019, below the value of 0.024 for the grid 4 case. The maximum levels of turbulence intensities at 65% chord for all cases are similar, ranging from 6.4% for the no-grid case to 7.0 to 7.4% for the three grids.

Conclusions

As might be expected, the transition location moved forward with each increase in turbulence intensity. It was found, though, that the boundary-layer with the most growth was not that of highest intensity. In order for freestream turbulence to affect turbulent boundary-layer behavior, the length scale must be on the order of the boundary-layer thickness. Grid 4, with an intensity of 0.5% and a dissipation length scale of 0.25 in., had a stronger effect on growth than grids 1 and 3, each with a much higher turbulence intensity, but also with a length scale an order of magnitude larger than the boundary-layer thickness.

The dependence of transitional behavior and boundary-layer growth on the freestream turbulence structure is not a simple one. Experiments documenting both turbulence intensity and length scale (or spectral content) will be necessary to provide data for verification of new turbulence models.

Acknowledgments

The support of the Naval Postgraduate School Research Council while conducting this research is gratefully acknowledged.

References

[1]Mueller, T. J., Pohlen, L. J., Conigliaro, P. E., and Jansen, B. J., Jr., "The Influence of Free-Stream Disturbances on Low Reynolds Number Airfoil Experiments," *Experiments in Fluids,* Vol. 1, No. 1, 1983, pp. 3–14.

[2]Marchman, J. F., "Aerodynamic Testing at Low Reynolds Numbers," *Journal of Aircraft,* Vol. 24, No. 2, 1987, pp. 107–114.

[3]Hall, D. J., and Gibbings, J. C., "Influence of Stream Turbulence and Pressure Gradient Upon Boundary Layer Transition," *Journal of Mechanical Engineering Science,* Vol. 14, No. 2, 1972, pp. 134–146.

[4]Hilsop, G. S., "The Transition of a Laminar Boundary Layer in a Wind Tunnel," Ph.D. Thesis, University of Cambridge, England 1940.

[5]Abu-Ghannam, B. J., and Shaw, R., "Natural Transition of Boundary Layers—The Effects of Turbulence, Pressure Gradient, and Flow History," *Journal of Mechanical Engineering Science,* Vol. 22, No. 5, 1980, pp. 213–228.

[6]Meier, H. U., and Kreplin, H.-P., "Influence of Freestream Turbulence on Boundary-Layer Development," *AIAA Journal,* Vol. 18, No. 1, 1980, pp. 11–15.

[7]Portfors, E. A., and Keffer, J. F., "Isotropy in Initial Period Grid Turbulence," *Physics of Fluids,* Vol. 12, No. 7, 1969, pp. 1519–1521.

[8]Hancock, P. E., and Bradshaw, P., "The Effects of Free-Stream Turbulence on Turbulent Boundary Layers," *Journal of Fluids Engineering,* Vol. 105, Sept. 1983, pp. 284–289.

[9]Castro, I. P., "Effects of Free Stream Turbulence on Low Reynolds Number Boundary Layers," *Journal of Fluids Engineering,* Vol. 106, Sept. 1984, pp. 298–306.

[10]Meier, H. U., "The Response of Turbulent Boundary Layers to Small Turbulence Levels in the External Free Stream," ICAS Paper 76-05, Oct. 1976.